CSCE Annual Conference

Growing with youth – Croître avec les jeunes

Laval (Greater Montreal)

June 12 - 15, 2019

STRUCTURAL STABILITY OF CONCRETE SPILLWAY PIERS: DEVELOPMENT AND APPLICATION OF 3D FIBER ELEMENTS INCLUDING SHEAR AND WARPING DEFORMATIONS

Do, V.T.[1,3], Léger, P.[2,4]
[1] Ph.D Candidate, Polytechnique Montreal, Canada
[2] Professor, Polytechnique Montreal, Canada.
[3]van-trung.do@polymtl.ca
[4] pierre.leger@polymtl.ca

Abstract:

This paper presents a new higher order 3D fiber element using beam theory leading to a 18x18-stiffness matrix including shear and torsional warping. This element is used to analyze the structural response of concrete spillway piers with deep variable cross-sections subjected to 3D loads. The element stiffness matrix is computed from numerical integration using a mixed formulation: (i) the flexibility method is used for flexural and shear influence coefficients; (ii) the displacement method is used for torsional influence coefficients (Saint–Venant and warping). The element (fibers) cross sections along the beam are first discretized at Gauss points using the 2D finite element method (FEM). The element stiffness matrix is then computed from Gauss integration of cross-sectional stiffness coefficients. This novel deep beam model allowing to consider combination of axial, bending, shear and torsional loads is implemented in a MATLAB code. A beam-column example for deep beam is considered to verify and validate the proposed model by comparisons with 3D ABAQUS finite element solutions using solid elements.

1 INTRODUCTION

Three-dimensional structural analysis methods for deep plain concrete spillway piers (Fig.1) subjected 3D loads (P-M_x-M_y-V_x-V_y-T) can be divided into three categories: (i) the gravity method; (ii) 3D fiber elements (Fig 1.b); and (iii) 3D finite element method (FEM). The gravity method (GM) is used frequently in engineering practice to analyse hydraulic structures. It is based on Euler – Bernoulli beam theory with the assumption that cross sections remain plane after deformation. However, nonlinear normal and shear stress distributions induced by cross-sectional warping are not captured. Element warping can be captured using 3D FEM using commercial software such as ABAQUS with solid elements. Yet, 3D FEM requires significant resources and complex post-processing to compute classical engineering stability indicators such as (i) sliding safety factor, (ii) position of force resultants, (iii) cracked area, and (iv) maximum compressive stresses. 3D fiber elements use conventional beam theory input parameters such as cross-sectional area (A), moments of inertia (I_x, I_y, I_{xy}), effective shear sectional areas (A_x, A_y, A_{xy}) and torsional constants (J, Γ). Higher order beam theories lead to more precise results than the GM but with less complexity than 3D FEM in terms of engineering resources and result interpretation to take decision about the adequacy of stability indicators as compared to dam safety guidelines requirements.

The first solution for “shear lag” effect was presented by Cowper (1966) to consider shear deformations in cross-sections using an effective shear area coefficient for rectangular cross-section. Gruttmann and Wagner (2001), and Pilkey (2002) extended this solution for arbitrary shaped cross-sections using Timoshenko’s beam theory by including shear deformations. However, the warping effect was not considered to compute normal stress distributions. Elastic stress analyses of cross sections with arbitrary geometry subjected to three-dimensional loads was presented by Stefan and Léger (2011). It included shear and torsional warping deformations. However, this solution considered the Euler-Bernoulli formulation in bending. The normal stress distributions at individual cross-section were computed without interactions from a cross section to another to form a structural element (Fig.1c). The application of this solution is adequate for individual cross-sections. For deep concrete beam sections, that will eventually be cracked, it is necessary formulate suitable 3D elements, aggregating cross-sectional behaviours along the element axis and to add the shear warping deformations to compute normal stress distributions.

In the oriented research software OpenSees (OS) (Mazzoni et al., 2006), there are some fiber elements available to analyze structural beams and frames subjected 3D loads. OS fiber elements are including shear deformations from Timoshenko theory but without shear and torsional warping effects. Le Corvec (2012) developed a slender 3D nonlinear fiber element using Timoshenko beam theory including local warping deformations from shear and torsion. Capdevielle et al. (2016) pursued this solution by using all FE mesh points in the cross-sections to formulate a beam-column element including shear and torsion warping deformations using the displacement method. However, the formulation did not have any independent parameters for shear and torsion such as added degrees-of-freedoms (DOFs). These parameters were introduced in research by Dikaros and Sapountzakis (2014a, 2014b, 2014c); Sapountzakis (2013); Sapountzakis and Dikaros (2015) using the boundary element method to compute shear and torsion warping deformations. However, their models focused on thin walls box cross-sections with elastic and composite elements. For hydraulic structures, it is necessary to develop a novel fiber element model to include shear and torsional warping deformations for deep cross-section and to later introduce the nonlinear material effects from concrete cracking and uplift water pressures (Fig.1).

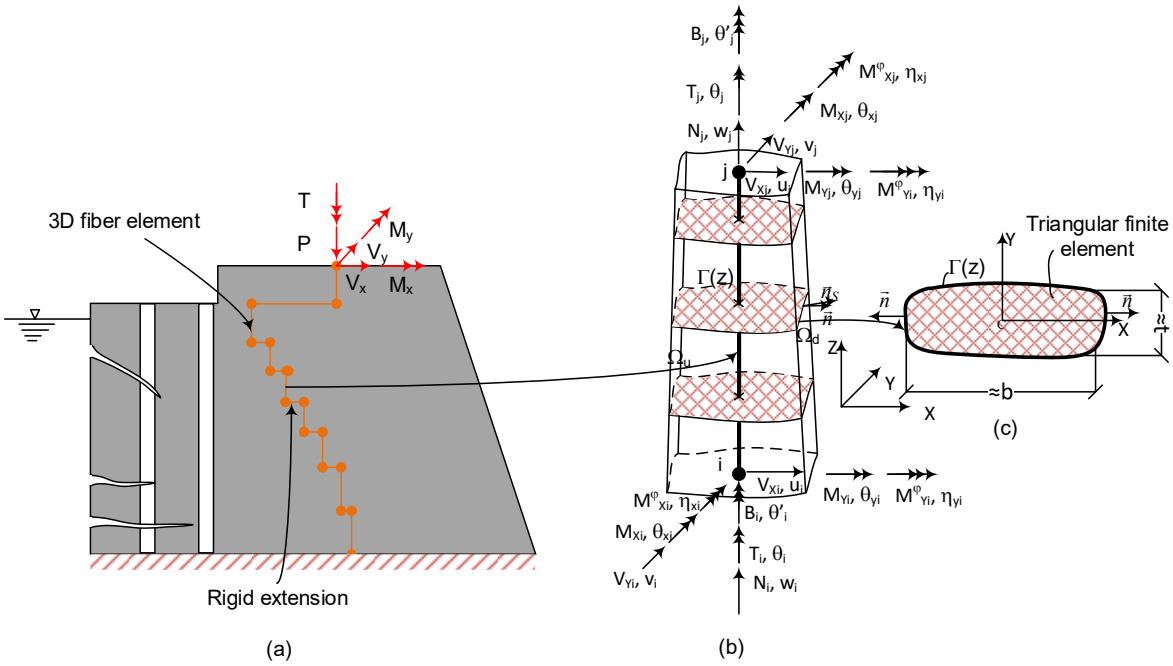

Figure 1: 3D Fiber beam-column element including non-uniform shear and torsion: (a) 3D fiber element model for spillway pier; (b) 3D fiber element parameters; (c) cross-section analyzed by 2D FEM.

This paper presents a new higher order 3D fiber element using deep beam theory leading to a 18x18-stiffness matrix including shear and torsion warping deformations. In Figure 1, each element has two nodes "i" and "j", with 9 DOFs per node. There are 6 DOFs for the usual translational and rotational displacements, and 2 added DOFs, η_X , η_Y , for shear warping displacements in X and Y directions, and 1 DOF, θ' , for torsional warping displacement associated with the Bi-moment, B (around Z). The element stiffness matrix is computed by using a mixed isoparametric formulation: (i) the flexibility method is used to compute flexural and shear influence coefficients; (ii) the displacement method is used to compute torsional influence coefficients (Saint–Venant and warping). This approach has some advantages for element with variable cross-sections. It is easier to work with force and equilibrium (flexibility) than to work with displacement and compatibility (stiffness) for P-M_x-M_y-V_x-V_y. For torsional effect, T, the bi-moment internal force-deformation relationship is described in the literature by the stiffness method. Herein torsional effect is thus considered using the displacement method by using Hermite polynomial functions to interpolate displacements along the element. The element (fibers) cross sections along the beam are first discretized using 2D FEM using triangular elements (Figure 1.c). The element stiffness matrix (from node "i" to "j") is then computed from Gauss integration of cross-sectional flexibility and stiffness matrix at Gauss points located along the element axis.

This 3D fiber element is implemented in a MATLAB code, named "*FIDAM*" using two formulations: (i) "Timoshenko" beam including torsional warping deformations leading to 14 DOFs and "FIDAM 18DOFs" including shear and torsion warping deformations. A geometrically complex concrete deep pier of a spillway is analyzed using ABAQUS (3D FEM) to validate the proposed fiber element model.

2 FINITE ELEMENT FORMULATIONS FOR SECTIONAL ANALYSIS

This section presents the finite element formulations for sectional analysis to compute sectional properties then, sectional stiffness or flexibility matrix. This matrix is computed from Gauss points along the element (Fig.2.I) including shear and torsional warping deformations.

The distribution of normal stresses on an arbitrary cross-section is given by:

$$\sigma_Z(x,y,z) = \sigma_z^p(x,y,z) + \sigma_z^w(x,y,z) \tag{1}$$

$\sigma_z^p(x,y,z)$: Linear normal stresses from Euler – Bernoulli beam theory;

$\sigma_z^w(x,y,z)$: Nonlinear normal stresses from shear and torsion warping deformations.

2.1 Sectional flexural stiffness matrix using Euler - Bernoulli

Euler - Bernoulli theory is used to determine the linear normal stresses and deformations to compute cross-section flexibility matrix (Fig. 2.I.a). The cross section is divided in a given number n_{fib} of sub-sections called fibers. The generic i-th fiber, of area A_{fibi}, is identified by means of the position of its centroid (x_{fibi}, y_{fibi}). The sectional stiffness matrix is first determined from equation (2) (Spacone et al., 1996) where I(x_{fibi}, y_{fibi}, z) is a geometric vector I(x_{fibi}, y_{fibi}, z) = {1 -x, y}, and E_{fibi} is the Young's modulus of i-th fiber.

$$\left[k_s(z)\right]_{3x3} = \sum_{i=i}^{n_{fib}(z)} I^T(x_{fibi}, y_{fibi}, z)_{3x1} (E_{fibi} A_{fibi})_{1x1} I(x_{fibi}, y_{fibi}, z)_{1x3} \tag{2}$$

The sectional flexibility matrix is obtained from the inverse of the sectional stiffness matrix: $\left[f_s^P(z)\right]_{3x3} = \left[k_s(z)\right]^{-1}{}_{3x3}$. For a symmetric cross-section, this matrix is diagonal from equation (3):

$$\left[f_S^P(z)\right]_{3x3} = \begin{bmatrix} 1/EA & 0 & 0 \\ 0 & 1/EI_{xx} & 0 \\ 0 & 0 & 1/EI_{yy} \end{bmatrix}_{3x3} \quad (3)$$

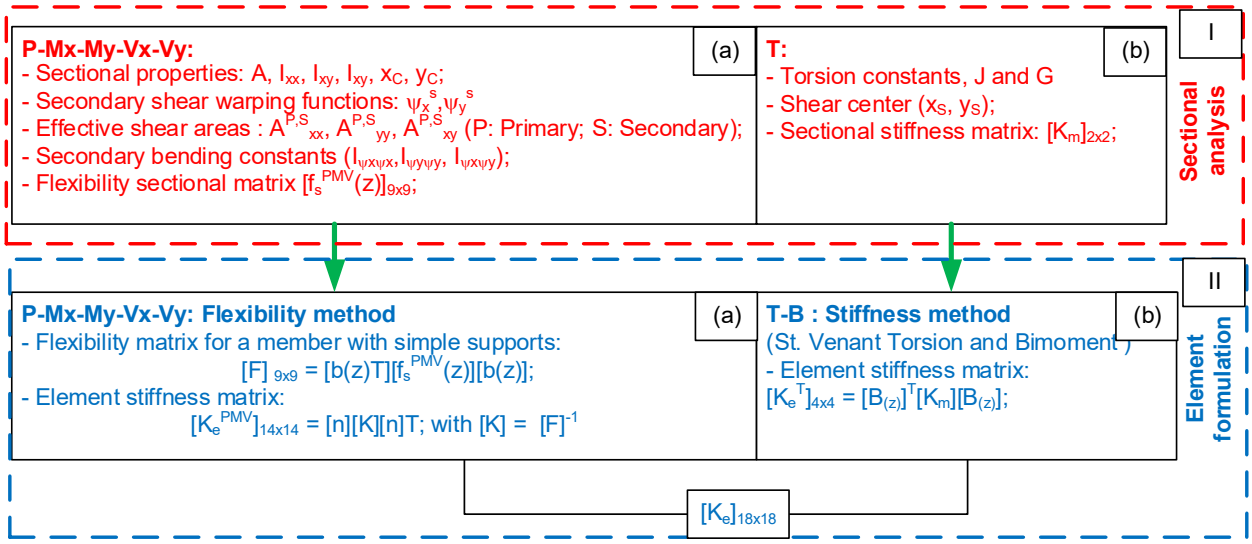

Figure 2: Element stiffness matrix formulations: (I) Step 1: Sectional flexibility and stiffness matrices; (II) Step 2: Element stiffness matrix formulation.

Model	Deformations	Shear stresses	Normal stresses	Equilibrium equation
a, Timoshenko beam theory b, Primary shear order	(a) (b)	+ $\tau_{xz}^P = G\gamma_x^P \psi_{x,x}^P$	$\sigma_z^P = \frac{M_Y}{I_y} x$	$\frac{\partial \tau_{xz}^p}{\partial x} + \frac{\partial \tau_{yz}^p}{\partial y} + \frac{\partial \sigma_z^p}{\partial z} = 0$ ψ_x^P: primary shear function
c, Secondary shear order	Secondary shear effect	+ $\tau_{xz}^S = G\gamma_x^S \psi_{x,x}^S$	+ $\sigma_z^w = \frac{M_Y^\psi}{I_{\psi\psi_x}} \psi_x^S$	$\frac{\partial \tau_{xz}^s}{\partial x} + \frac{\partial \tau_{yz}^s}{\partial y} + \frac{\partial \sigma_z^w}{\partial z} = 0$
d, Proposed model (FIDAM-18DOFs)	Total deformations	II $\tau_{xz} = \tau_{xz}^P + \tau_{xz}^S$	II $\sigma_z = \sigma_z^p + \sigma_z^w$	Secondary shear function: $\psi_x^S = \psi_x^P - X$

Figure 3: Modelling of shear deformations and related normal stresses (V_x only): (a) Timoshenko beam theory; (b) Primary shear order; (c) Secondary shear order; (d) Proposed model for shear effect in FIDAM – 18DOFs.

2.2 Sectional stiffness matrix including shear warping deformations

The shear sectional stiffness matrix is used to determine shear stresses and deformations by using 2D FEM to compute primary and secondary warping functions. The primary warping functions are used (Stefan and Léger, 2011) to compute primary shear stresses and effective shear area coefficients. The secondary warping functions are developed from Dikaros and Sapountzakis (2014b) to compute secondary shear and normal stresses.

- **Primary shear warping function**

Stefan and Léger (2011) used shear warping functions to solve the shear stress distribution by 2D FEM for elastic variable cross-section element. This solution is based on the elasticity theory with a Poisson differential equation by using proper boundary conditions. In equation (4), $\psi_G(x,y,z)$ is the primary warping functions, with $\psi_X^P(x,y,z)$ and $\psi_Y^P(x,y,z)$ for x, and y directions. The function, $f(x,y)$, is a normal stress function along of the element length. The Poisson differential equation is given by ($\psi_G = \psi \cdot G$), with G = E/2/(1+ν), v being the Poisson ratio and E being the elastic modulus:

$$\left(\frac{\partial \tau_{xz}^p}{\partial x} + \frac{\partial \tau_{yz}^p}{\partial y} + \frac{\partial \sigma_z^p}{\partial z} \right) \Bigg|_{z=zi} = 0 \qquad \Rightarrow \qquad -\nabla^2 \psi_G = f(x,y)\big|_{z=zi} \tag{4}$$

The primary shear stresses in the section z_i are computed from:

$$\tau_{xz\,S}^p = \frac{\partial \psi_G}{\partial x} + h_{nx}; \qquad \tau_{yz\,S}^p = \frac{\partial \psi_G}{\partial y} + h_{ny} \tag{5}$$

with h_{nx} , h_{ny} being functions depending on the boundary conditions (Stefan and Léger, 2011). Herein, we used the solution of Pilkey (2002) to compute the shear centre location (x_D, y_D), shear deformation coefficients (α_{xx}, α_{yy}, α_{xy}) from Timoshenko beam theory, and primary shear areas (A_X^P, A_Y^P, A_{XY}^P) to build the sectional stiffness matrix.

- **Secondary shear warping function**

The shear lag effect in deep cross-sections can be captured by using secondary order shear warping functions (Figure 3). Dikaros and Sapountzakis (2014c) developed a secondary shear warping function from the third equation of elasticity theory. For a rectangular cross-section, the secondary shear warping functions ($\psi_X^s(x,y,z)$, $\psi_Y^s(x,y,z)$) are obtained from the primary shear warping functions from equation (6). Two independent parameters are defined for secondary shear warping DOFs (η_X , η_Y), along the axes x, y.

$$\psi_X^s(x,y,z) = \psi_X^p \frac{A_X^P}{V_x} - x; \quad \psi_Y^s(x,y,z) = \psi_Y^p \frac{A_y^P}{V_Y} - y \tag{6}$$

The secondary normal and shear stresses are obtained from equation (8). Secondary shear average deformations (γ_X^S , γ_Y^S) are computed from primary shear deformations and secondary displacements, $\gamma_X^S = \eta_Y - \frac{V_X^P}{A_X^P}; \gamma_Y^S = \eta_X - \frac{V_Y^P}{A_Y^P}$ (Dikaros and Sapountzakis, 2014c). Due to the development of normal stresses, there are also three secondary sectional inertia moment properties ($I_{\psi_X\psi_X}$, $I_{\psi_Y\psi_Y}$, $I_{\psi_X\psi_Y}$) in analogy to the sectional moments of inertia in bending (I_{xx}, I_{yy}, I_{xy}).

$$I_{\psi_x\psi_x} = \int_A (\psi_X^S)^2 dA; \quad I_{\psi_y\psi_y} = \int_A (\psi_Y^S)^2 dA; \; I_{\psi_x\psi_y} = \int_A \psi_X^S \psi_Y^S dA; \tag{7}$$

$$\sigma_z^w = EI_{\psi_x\psi_x} \frac{d\eta_Y}{dz} \psi_x^s(x,y,z) + EI_{\psi_y\psi_y} \frac{d\eta_X}{dz} \varphi_y^s(x,y,z) \tag{8}$$

$$\tau_{xz}^w = G\gamma_x^s \psi_{x,x}^s(x,y,z) + G\gamma_y^s \psi_{y,x}^s(x,y,z); \; \tau_{yz}^w = G\gamma_y^s \psi_{x,y}^s(x,y,z) + G\gamma_y^s \psi_{y,y}^s(x,y,z)$$

For the shear sectional stiffness matrix to include shear lag effects, we have to consider secondary shear areas in equation (9). In this paper, we neglect the coupling term A^S_{XY} :

$$A_X^s = A - A_X^P; \quad A_Y^s = A - A_Y^P; \quad A_{XY}^s = 0 \tag{9}$$

The shear sectional stiffness matrix, $\left[k_s^{VV}\right]_{4\times4}$ and the secondary bending sectional matrix, $\left[k_s^{M\psi}\right]_{2\times2}$ in equation (10) are given below :

$$\left[k_s^{VV}\right]_{4\times4} = \begin{bmatrix} GA_X^p & GA_{XY}^p & 0 & 0 \\ GA_{XY}^p & GA_Y^p & 0 & 0 \\ 0 & 0 & GA_X^s & 0 \\ 0 & 0 & 0 & GA_Y^s \end{bmatrix}; \quad \left[k_s^{M\psi}\right]_{2\times2} = \begin{bmatrix} EI_{\psi_x\psi_x} & EI_{\psi_x\psi_y} \\ EI_{\psi_x\psi_y} & EI_{\psi_y\psi_y} \end{bmatrix} \tag{10}$$

To obtain the sectional flexibility matrix including shear lag and secondary bending effects, we invert $\left[k_s^{VV}\right]_{4\times4}$ and $\left[k_s^{M\psi}\right]_{2\times2}$. The sectional flexibility matrix for axial-shear-bending effects is then:

$$\left[f_s^{PMV}(z)\right]_{9x9} = \begin{bmatrix} \left[f_s^P(z)\right]_{3x3} & 0 & 0 \\ 0 & \left[f_s^{VV}(z)\right]_{4x4} & 0 \\ 0 & 0 & \left[f_s^{M\psi}(z)\right]_{2x2} \end{bmatrix}_{9\times9} \tag{11}$$

2.3 Sectional stiffness matrix including torsion warping deformations

Torsion sectional formulation is based on the solution of Stefan and Léger (2011) including two effects: (1) the Saint – Venant (uniform) torsion when the section is free to warp ; (2) the warping (non-uniform) torsion when sectional warping is restrained. This problem is solved in two steps: (1) computation of Saint-Venant torsional shear stresses and torsional constant (J); (2) computation of the warping effect and the torsional warping constant (Γ).

The torsional cross-sectional stiffness matrix including the torsional warping deformations is given by:

$$\left[k_s^{TB}\right]_{2\times2} = \begin{bmatrix} EJ & 0 \\ 0 & E\Gamma \end{bmatrix} \tag{12}$$

3 THREE-DIMENSIONAL ELEMENT STIFFNESS MATRIX FORMULTATION

This section presents the formulation of the 18x18 element stiffness matrix for 3D fiber element including shear and torsional warping deformations (Fig2.II). There are two methods to obtain this element stiffness matrix: (1) the flexibility method for P-M_x-M_y-V_x-V_y that is shown in Figure 2.II.a ; (2) the stiffness method for torsion that is presented in Figure 2.II.b.

3.1 Flexibility method (P-V-V-M-M)

The flexibility method is based on force interpolation functions along a simply supported 3D element. These functions, $\left[b(z)\right]_{9\times9}$ are obtained by applying unit loads at each DOF and from the differential relations between shear forces and bending moments in equation (13). In a first step, we can obtain the flexibility matrix of a 3D simply supported element, $\left[F\right]_{9x9}$ in equation (14).

$$V_X = V_X^P + V_X^S; \quad V_Y = V_Y^P + V_Y^S; \frac{dM_X}{dz} = V_Y; \quad \frac{dM_y}{dz} = V_X \tag{13}$$

$$\left[F\right]_{9x9} = \int_0^L \left[b(z)\right]_{9\times9}^T \left[f_s^{PMV}(z)\right]_{9x9} \left[b(z)\right]_{9x9} dz \tag{14}$$

Then, the stiffness matrix of 3D element can be obtained by inverting the flexibility matrix, $K = \left[F\right]^{-1}_{9x9}$. A transformation matrix, $\left[n\right]$, is then applied to obtain the complete set of forces from the reduced set where free body motions have been prevented (for more details see Vu-Quoc and Léger (1992), Neuenhofer and Filippou (1998)):

$$\left[K_e^{PMV}\right]_{14\times14} = \left[n\right]\left[K\right]\left[n\right]^T \tag{15}$$

3.2 Stiffness method (Torsion)

The stiffness method is based on displacement interpolation functions. In this paper, Hermite cubic polynomials, $\left[H(z)\right] = \left[H_1(z) \quad H_2(z) \quad H_3(z) \quad H_4(z)\right]$, are used to compute the torsion element matrix, $\left[K_e^T\right]_{4\times4}$, including Saint-Venant and warping torsion.

$$\begin{aligned} H_1(z) &= 1 - \frac{3z^2}{L^2} + \frac{2z^3}{L^3}; H_2(z) = z - \frac{2z^2}{L} + \frac{z^3}{L^2} \\ H_3(z) &= -\frac{2z^3}{L^3} + \frac{3z^2}{L^2}; H_4(z) = \frac{z^3}{L^2} - \frac{z^2}{L} \end{aligned} \tag{16}$$

Based on the deformation – displacement relations, we have equation:

$$\varepsilon(x,y,z) = \left[B(z)\right]\left\{u^e\right\} \tag{17}$$

Where $\left\{u^e\right\} = \left[\theta_i \quad \theta_j \quad \theta_i^{'} \quad \theta_j^{'}\right]^T$ is the nodal displacement vector, $\theta(z) = \left[H(z)\right]\left\{u^e\right\}$ is the angle of rotation along the element axe and $\varepsilon(x,y,z)$ are sectional deformations. The displacement interpolation functions are obtained from:

$$\left[B(z)\right] = \left[\frac{dH(z)}{dz}; \quad \frac{d^2H(z)}{dz^2}\right] \tag{18}$$

The element stiffness matrix in torsion is obtained from:

$$\left[K_e{}^T\right] = \int_0^L \left[B(z)\right]^T \left[k_s^{TB}(z)\right]\left[B(z)\right]dz \tag{19}$$

The 3D element stiffness matrix including shear and torsion warping deformations is presented in equation (20). For a structure that has variable cross-sections along of the element length, an element with rigid end offset extensions is used by applying an eccentricity matrix transformation.

$$\left[K_e\right]_{18\times18} = \begin{bmatrix} \left[K_e{}^{PMV}\right]_{14\times14} & 0 \\ 0 & \left[K_e{}^T\right]_{4\times4} \end{bmatrix}_{18\times18} \tag{20}$$

4 APPLICATION EXAMPLE AND NUMERICAL RESULTS

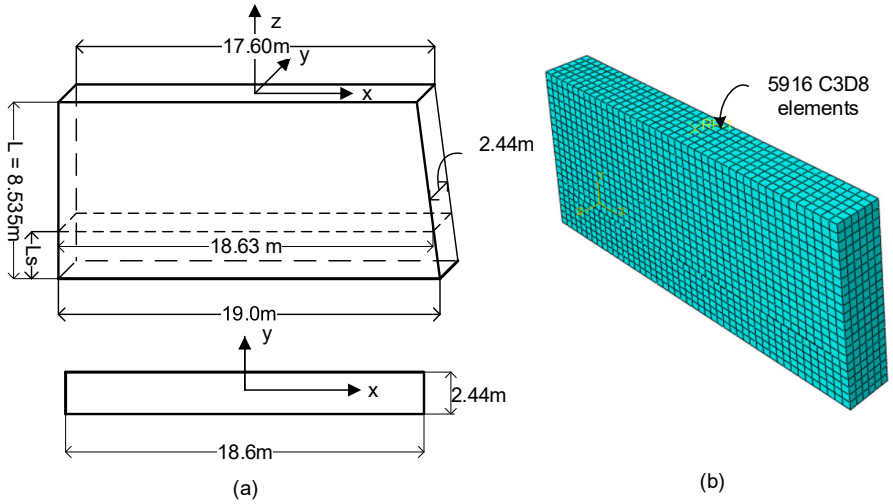

Figure 4: Application example: (a) variable spillway piers (squat wall – deep beam); (b) 3D FEM from ABAQUS with 5916 solid elements.

This example is a variable spillway pier (deep beam) shown in Figure 4.a. The material parameters are the Young modulus E_c = 30000 MPa, ν = 0. In this paper, Poisson effect is ignored to easily validate proposed model with ABAQUS using 3D solid FE. This spillway pier is subjected two load cases: (1) P = -2000 kN and V_x = 3000 kN; (2) Torsion (T = 200 kN.m). The results for the cross-section located at Ls = 2.254m are shown in Figure 5. In Figure 4.c1, the FIDAM displacement, u_x, along of the spillway pier, was shown to be similar to results using Timoshenko beam theory and 3D FEM (ABAQUS). The normal stress distribution for the first load case is obtained by using the proposed model, "*FIDAM-18DOFs*". It is nonlinear, and it exhibits a small error with a maximum ratio $\sigma_{FIDAM}/\sigma_{ABAQUS}$ = 1.007 for maximum compressive normal stresses. Overall, "*FIDAM-18DOFs*" shear stress distribution is very similar to the ABAQUS solution for the deep cross-sections with some local differences mainly at the sloped pier extremity (shown in Figure 4.a).

The second load case is a torsional moment, T = 200 kN.m. The rotational displacements along the structure height are showed in Figure 5.c2. "*FIDAM-18DOFs*" maximum rotation is very close to the ABAQUS solution. The normal and shear stress distributions are shown in Figure 5.b. They exhibit an acceptable error with a maximum ratio $\sigma_{FIDAM}/\sigma_{ABAQUS}$ = 1.13 (13% different). This error is caused by secondary torsional warping effect. We ignore the secondary shear order effect due to torsional load to compute normal stresses in the proposed model to avoid adding more DOFs and complexify further the element formulation and still provide reasonable stress estimate. The shear stress distributions from "*FIDAM-18DOFs*" are very similar to the ABAQUS solution for deep cross-section.

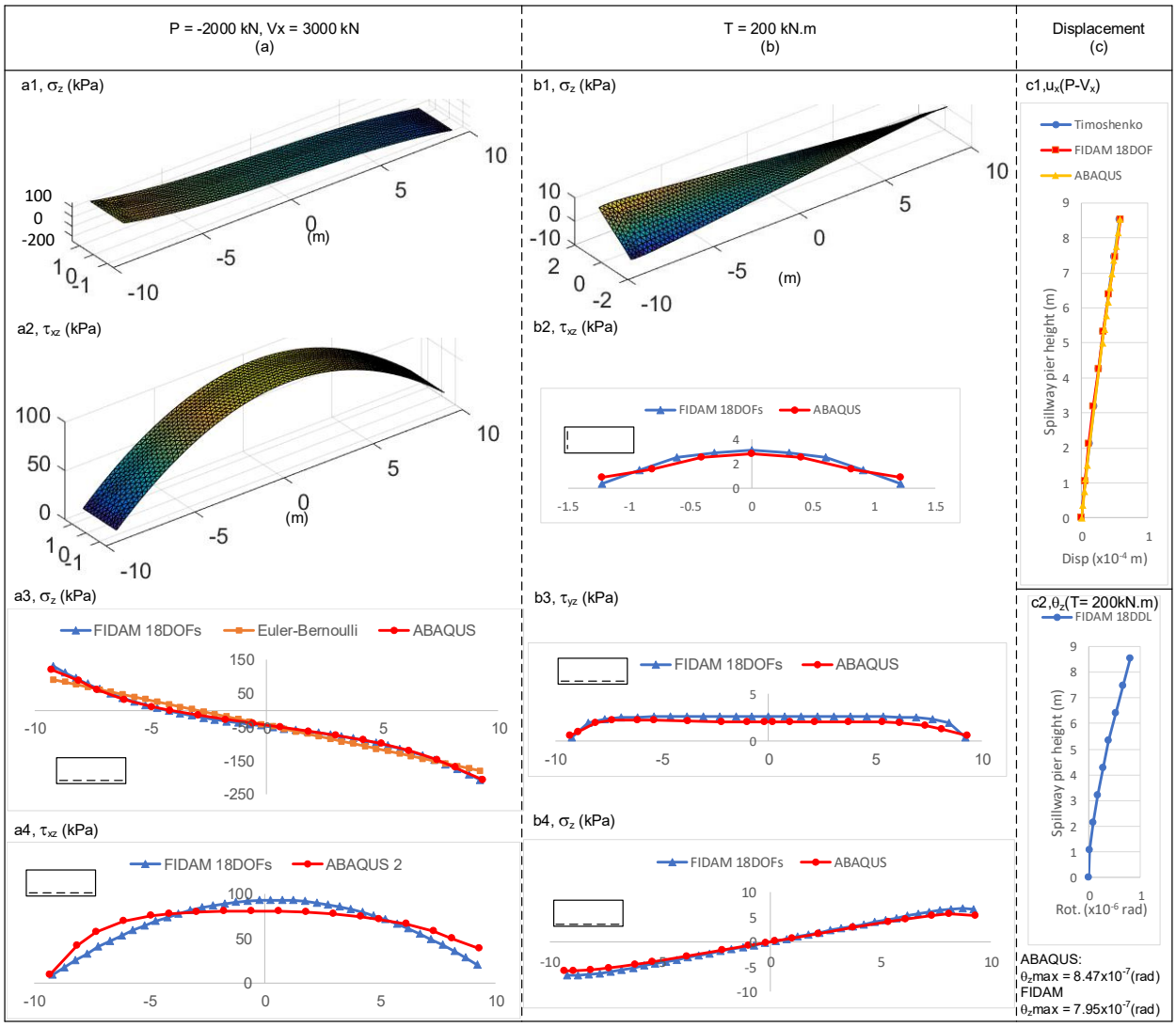

Figure 5: Results of spillway pier: (a) Stress distributions for P-V_x; (b) Stress distribution for T; (c) Displacements: c1 – translation u_x for P-V_x, c2-rotation for T.

5 CONCLUSIONS and RECOMMENDATIONS

This paper presents a novel fiber element model for deep elastic piers subjected to three-dimensional loads (axial force, biaxial shear forces, bending moments, and torsion). This fiber element has a 18x18 stiffness matrix dimension to include shear warping and torsional warping cross-sectional deformations. This model consists in the determination of the nonlinear normal and shear stress distributions for deep spillway piers by considering secondary shear and primary torsional effects (St-Venant, warping). An application example for rectangular spillway pier (squat wall) was presented. The main conclusions are as follows:

(a) The 3D fiber element model labeled as “FIDAM 18DOFs” presents nonlinear normal stress distributions for deep beam subjected to shear forces that are more representative than the linear stresses from classical Euler-Bernoulli beam theory and closely matched the 3D FE solution using solid elements from ABAQUS (within 1% error for maximum stresses).

(b) The fiber element model is implemented using a 2D+ efficient formulation to introduce shear and torsion warping deformations for squat structures subjected to axial, bending, non-uniform shear and

non-uniform torsion. The sectional analysis employs only some cross-sectional 2D surface meshes by using triangular FE to compute all necessaries sectional properties (primary and secondary).

(c) The “FIDAM” shear stress distributions are very similar to those from ABAQUS solution.

(d) This proposed beam-column model provides the framework to extend the formulation to include material nonlinearity such as concrete cracking, and uplift pressures to analyse efficiently spillway piers.

This study provided a frame work to implement advanced beam theory to analyse deep spillway piers. It is recommended to investigate the structural significance of shear and torsional distortions for deep concrete sections. It was shown herein that deep beam theory maximum tensile normal stresses is 45% larger, while the average value is 20% larger, than classical Euler Bernoulli solution.

Acknowledgements

This research has been co-financed by the Vietnamese Government’s Scholarship (Project 911), the Quebec Fund for Research on Nature and Technology, and the Natural Science and Engineering Research Council of Canada.

References

Capdevielle, S., Grange, S., Dufour, F., & Desprez, C. 2016. A Multifiber Beam Model Coupling Torsional Warping and Damage for Reinforced Concrete Structures. *European Journal of Environmental and Civil Engineering*, **20**(8): 914-935.

Cowper, G. R. (1966). The Shear Coefficient in Timoshenko's Beam Theory. *Journal of Applied Mechanics*, **33**(2): 335-340.

Dikaros, I., & Sapountzakis, E. 2014a. Generalized Warping Analysis of Composite Beams of An Arbitrary Cross Section by BEM. I: Theoretical Considerations and Numerical Implementation. *Journal of Engineering Mechanics*, **140**(9): 04014062.

Dikaros, I., & Sapountzakis, E. 2014b. Generalized Warping Analysis of Composite Beams of An Arbitrary Cross Section by BEM. II: Numerical Applications. *Journal of Engineering Mechanics*, **140**(9): 04014063.

Dikaros, I., & Sapountzakis, E. 2014c. Nonuniform Shear Warping Effect in the Analysis of Composite Beams by BEM. *Engineering Structures*, **76**(Supplement C): 215-234.

Gruttmann, F., & Wagner, W. 2001. Shear Correction Factors in Timoshenko's Beam Theory for Arbitrary Shaped Cross-sections. *Computational Mechanics*, **27**(3): 199-207.

Le Corvec, V. 2012. Nonlinear 3D Frame Element with Multi-axial Coupling under Consideration of Local Effects. Retrieved from http://www.escholarship.org/uc/item/0sw164c3

Mazzoni, S., McKenna, F., Scott, M. H., & Fenves, G. L. 2006. OpenSees Command Language Manual. Pacific Earthquake Engineering Research (PEER) Center.

Neuenhofer, A., & Filippou, F. C. 1998. Geometrically Nonlinear Flexibility-Based Frame Finite Element. *Journal of Structural Engineering,* **124**(6): 704-711.

Pilkey, W. 2002. *Analysis and Design of Elastic Beams–Computational Methods*, John Wiley & Sons, New York, USA.

Sapountzakis, E. 2013. Bars under Torsional Loading: A Generalized Beam Theory Approach. ISRN Civil Engineering, 2013: 1-39.

Sapountzakis, E., & Dikaros, I. 2015. Advanced 3D Beam Element of Arbitrary Composite Cross-section Including Generalized Warping Effects. *International Journal for Numerical Methods in Engineering*, **102**(1): 44-78.

Spacone, E., Filippou, F. C., & Taucer, F. F. 1996. Fiber Beam – Column Model for Non-linear Analysis of R/C Frames: Part I. Formulation. *Earthquake Engineering & Structural Dynamics*, **25**(7): 711-725.

Stefan, L., & Léger, P. 2011. Elastic Sectional Stress Analysis of Variable Section Piers Subjected to Three-dimensional Loads. *Computers & Structures,* **90-91**: 28-41.

Vu-Quoc, L., & Léger, P. 1992. Efficient Evaluation of the Flexibility of Tapered I-Beams Accounting for Shear Deformations. *International Journal for Numerical Methods in Engineering,* **33**(3): 553-566.